doi: 10.1111/j.1365-3121.2006.00705.x

Fault slip and Coulomb stress variations around a pressured magma reservoir: consequences on seismicity and magma intrusion

J. Gargani,[1] L. Geoffroy,[1] S. Gac[2] and S. Cravoisier[1,3]

[1]*LGRMP, University of Maine, Le Mans 72085, France;* [2]*Department of Earth Science, University of Bergen, Norway;* [3]*EOST, University of Strasbourg 1, France*

ABSTRACT

Pressure variations in a magma reservoir may cause deformation at the surface and a redistribution of the stress in the surrounding rock. In this study, we use two-dimensional numerical models and elaborate how magma chamber inflation and deflation affect the stress field around and surface displacement. We test how a pre-existing normal fault near the magma reservoir may influence the pattern of stress. We demonstrate the possibility of initiating both normal and reverse slip on faults during the inflation of the magma reservoir. The Coulomb failure stress changes are calculated during the periods of pressure variation. An increase of Coulomb failure stress can be predicted above and below the magma chamber during increasing magma chamber pressure that may encourage earthquakes. This process can produce cracks and fault growth encouraging magma propagation along the cracked zone. A different distribution of the stress change is expected in the case of subsequent deflation of the overpressured magma reservoir. In this case, seismicity is expected on a plane at equal depth than the magma chamber, laterally offset from the extent of the magma chamber. Magma could propagate laterally from the magma reservoir into zones where cracks have been generated, but only if the resolved shear stress on the fault is small compared with the excess magma pressure.

Terra Nova, 18, 403–411, 2006

Introduction

Over the past two decades, numerous studies have investigated the relationship between volcanic activity and seismicity (e.g. Tilling and Dvorak, 1993; Troise, 2001; Toda *et al*., 2002; Doubre, 2004; Foulger *et al*., 2004, 2005; Walter and Amelung, 2004). An increase of seismicity above the magma reservoir of Campi Flegrei (Italy) is believed during inflation of the magma reservoir (De Natale and Zollo, 1986; De Natale *et al*., 1995). Also during inflation, Tilling and Dvorak (1993) observed seismicity above and below the magma reservoir of the Kilauea volcano (Hawaii). The seismicity has been less studied during deflation of magmatic chamber. In this case, the location of seismicity is unclear. Nevertheless, before the Loihi seamount (Hawaii) collapse, seismicity was located laterally offset from the extent of the magma chamber (Caplan-Auerbach and Duennebier, 2001).

Correspondence: Dr Julien Gargani, Laboratoire de Geodynamique des Rifts, Universite du Maine, Avenue Olivier Messiaen, 72085 Le Mans, France. Tel.: +33 2 43 83 32 38; fax: +33 2 43 83 37 95; e-mail: julien.gargani@univ-lemans.fr

In volcanic areas, it is necessary to distinguish between seismic activity generated by tectonic processes (short-period waves) and seismic activity provoked by fluid propagation (short-period and long-period waves, volcanic tremors). A complete time-history analysis of seismicity preceding and accompanying volcanic eruptions is required to understand the interplay between tectonic and magmatic processes. Unfortunately, it is not always possible to do this, especially with old data. Under these conditions, it is difficult to interpret adequately the observed phenomena.

Fault and boundary fractures are believed to play a role in the evolution of magma reservoir. This role is difficult to interpret because the activity of fault is often contemporaneous with magma chamber activity. The relation between the magma chamber activity and the seismic activity is considered as evidence of stress change (Troise *et al*., 1997). Recently, Troise *et al*. (2003) have shown that the seismicity at the Campi Flegrei caldera is matching areas of increased Coulomb failure stress above the pressure source, nearby a fault, during magma reservoir inflation. It has also been suggested that earthquakes could trigger eruptions (Nostro *et al*., 1998; Hill *et al*., 2002).

Previous researches have studied separately magma chamber activity, fault slip, seismicity and magma propagation. Furthermore, the effect of deflation on stress change has not been studied in detail. The aim of this study was to improve our understanding of seismic activity in volcanic areas, in terms of both location and processes. We would like to understand how magma reservoir activity is able to produce deformation which allows magma propagation along preferential direction. A numerical approach is applied to model the pressure variations of a magma reservoir near a pre-existing fault. In this study, we tested and discuted the influence of: (1) the effects of varying magma chamber pressure (increase and decrease) on ground surface movements and displacements across pre-existing faults; (2) the variation in magma chamber pressure on the location of micro-seismicity; (3) the possible consequences on magma injection from the magma reservoir.

Coulomb stress change theory

Several studies have shown that static stress changes as small as 0.01 MPa

caused by large earthquakes may trigger subsequent events in a crust close to the critical state of failure (Stein, 1999). Such a relationship between stress change and aftershock location has been demonstrated using the Coulomb failure stress change (King *et al.*, 1994). Failure occurs when the change in Coulomb failure stress ($\Delta\sigma_f$) exceeds a threshold value (Stein, 1999). The Coulomb failure stress change $\Delta\sigma_f$ is defined by:

$$\Delta\sigma_f = \Delta\tau_0 + \mu(\Delta\sigma_n + \Delta p) \quad (1)$$

where $\Delta\tau_0$ is the shear stress change parallel to the fault slip (positive if having the same sign), $\Delta\sigma_n$ is the change in normal stress (positive for extension), Δp is the pore pressure change and μ is the frictional coefficient ranging from 0.6 to 0.85 (Byerlee, 1978). We use $\mu = 0.75$ in the modelling study presented here. The change in pore pressure due to a change in stress is given by:

$$\Delta p = -\frac{B}{3}\Delta\sigma_{kk} \quad (2)$$

where $\sigma_{kk} = \sigma_{xx} + \sigma_{yy} + \sigma_{zz}$ is the volumetric stress and B is the Skempton coefficient. We adopt a value of $B = 0.5$ (Árnadóttir *et al.*, 2003).

Model procedure

A finite element model was constructed to evaluate the rate of stress change in a faulted crust following pressure variation within a magma chamber. All models incorporate (see Fig. 1): (1) a crust (continental or oceanic) with a thickness of 30 km and having a viscoelastic rheology; (2) a spherical magma chamber (Gudmundsson *et al.*, 1997) at a depth of 3.5 or 6 km, with an internal temperature of 1100 °C and a radius of 1 km; (3) a planar fault dipping between 60° and 80° located at various distances from the magma chamber.

The lithosphere is modelled by a two-dimensional viscoelastic model with two layers. The crust is 30 km thick and 100 km in length (Fig. 1A). The continental crust usually has a thickness of 30 km. Such values can also be observed for oceanic crust in areas such as Iceland where there is increased mantle melting (Foulger *et al.*, 2003). A thickness of 25 km of the mantle lithosphere is modelled.

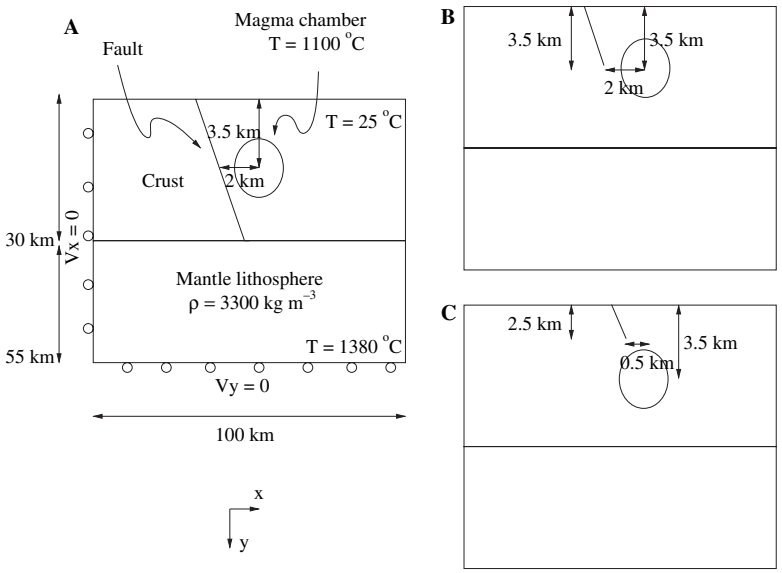

Fig. 1 Main features of the numerical model. The different fault lengths are simulated as well as the various positions of the fault in relation to the magma chamber. (A) The fault passes to one side of the magma chamber, and the maximum depth of the fault is 30 km. (B) Same as in A, but the maximum depth of the fault is 3.5 km. (C) The fault originates above the roof of the magma chamber. Not to scale.

The base of the model (55 km) has a temperature of 1380 °C. Foulger *et al.* (2004, 2005 have estimated a temperature of 1300 °C at 50 km depth. We focus our study on the upper part of the crust where a magma reservoir is simulated at a temperature of 1100 °C. This corresponds to melt temperature (De Natale *et al.*, 2004). The surface temperature is 25 °C. We assume a magma reservoir radius of 1 km at various depths (3.5 and 6 km). For active magma chambers, the volumes are estimated at 5–500 km^3 which, for a spherical chamber, would indicate a radius of ~1–5 km (Gudmundsson and Brenner, 2004). The depths tested in our model for the magma reservoir are of the same order as the estimation of magma reservoir depth at Campi Flegrei, which has been estimated to be below 4 km (De Natale and Pingue, 1993; Beauducel *et al.*, 2004) and at 3.5–4 km depth for the Mauna Loa (Hawaii) (Walter and Amelung, 2004).

All the modelling presented here was carried out using the finite element model Ansys (http://www.ansys.com). Our model allows us to estimate the magnitude of the following parameters: ground deformation, fault slip, $\Delta\tau_0$, $\Delta\sigma_n$ and $\Delta\sigma_{kk}$.

Rheology modelling

To model satisfactorily the stress fields and deformation around a crustal magma chamber, we need to take into account the mechanical properties of the whole lithosphere. In particular, the continental or oceanic rheology of the crust is expected to play a non-negligible role and must be considered along with the viscous effect. Viscous relaxation may redistribute stresses in the crust over time after a localized stress change (Parsons, 2002). This process allows to interpret post-rifting deformation in a volcanic rift zone (Cattin *et al.*, 2005).

The mode of deformation (i.e. elastic or viscous) depends on rock composition, temperature and strain rate. In the lithosphere, nonlinear creep processes prevail at high temperatures. The relation between stress and strain rate is calculated from:

$$\dot{\varepsilon} = A\sigma^n \exp\left(-\frac{Q}{RT}\right) \quad (3)$$

where $\dot{\varepsilon}$ is the strain rate, A, n and Q are, respectively, the viscosity parameter, the power exponent and activation energy derived from laboratory experiments, while R is the universal gas constant, T is the temperature and σ is the differential stress ($\sigma_1 - \sigma_3$)

Table 1 A and n are two experimental constants, Q is the activation energy, E is Young's modulus, ν is Poisson's ratio, k is the thermal diffusivity and ρ is the density.

Parameter	Oceanic crust (0–30 km)		Continental crust (0–30 km)		Mantle (30–55 km)	
A (Pa^{-n} s^{-1})	1.0×10^{-21}	1	3.16×10^{-26}	5	2.41×10^{-16}	2
Q (kJ mol^{-1})	230	1	186.5	5	540	2
n	3.0	1	3.3	5	3.5	2
E (Pa)	5×10^{10}	3	5×10^{10}	3	7×10^{10}	3
ν	0.25	4	0.25	4	0.25	4
k (W m^{-1} K^{-1})	2.6	4	2.6	4	2.6	4
ρ (kg m^{-3})	2900	4	2700	4	3300	4

References for viscosity parameters: (1) metagabbro, Cheng *et al.* (2002); (2) dry olivine, Karato and Wu (1993); (3) Pascal and Cloething (2002); (4) Huismans *et al.* (2001); (5) van Wijk and Cloething (2002).

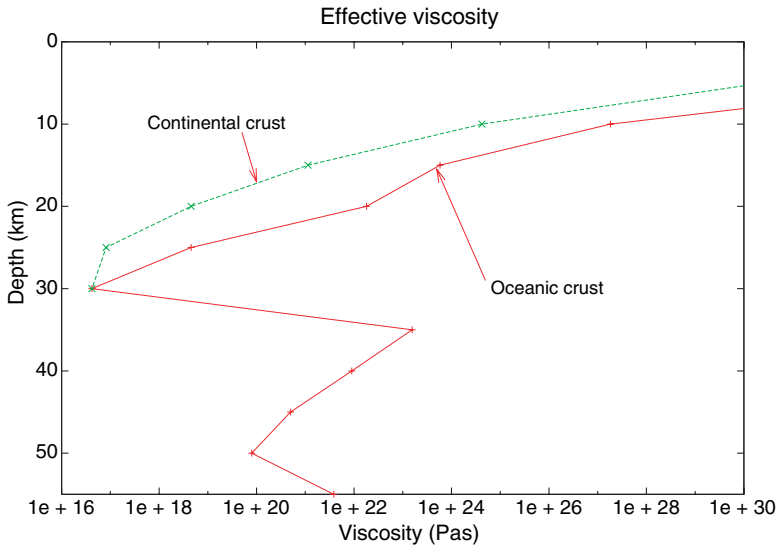

Fig. 2 Effective viscosity vs. depth. Viscosity is calculated from the equation $\mu = [\sigma^{1-n} \exp(Q/RT)]/2A$, where σ is the differential stress $\sigma_1 - \sigma_3$ (calculated with the finite element model), R is the gas constant, Q is the activation energy, while A and n are experimentally determined values (see Table 1).

(Turcotte and Schubert, 2002). A metagabbro rheology (Wilks and Carter, 1990 cited in Cheng *et al.*, 2002) is assumed to simulate the oceanic crust. The continental crust is simulated by adopting the parameters for granite (van Wijk and Cloething, 2002). Lithospheric mantle is simulated by dry olivine rheology (Karato and Wu, 1993) (see Table 1 for values).

The resulting lithosphere has a high viscosity in its uppermost part (Fig. 2), as usually obtained with numerical models (Bokelmann and Silver, 2002). Continental crust is easier to deform than oceanic crust. The low viscosity of the oceanic lower crust (Fig. 2) is in agreement with the viscosity of the oceanic crust beneath Iceland, estimated at between 3×10^{17} and 5×10^{19} Pa s (Hofton and Foulger, 1996), as well as with the viscosity value of $0.5–1 \times 10^{18}$ Pa s estimated for the Afar transitional crust (Cattin *et al.*, 2005).

Fault modelling

In rift zones, the dips of normal faults are in the range 60–80° for continental (Micarelli *et al.*, 2003; Cornu and Bertrand, 2005), intermediate (Doubre, 2004; Cattin *et al.*, 2005) or Icelandic-type crust (Angelier *et al.*, 1997; Grant and Kattenhorn, 2004; Gudmundsson and Loetveit, 2005). We tested several positions of the fault, with various geometries and lengths (Fig. 1).

The fault is deformable and is constructed from contact elements governed by the Coulomb failure relation:

$$\tau_f = \tau_0 + \mu\sigma_n \quad (4)$$

where μ is the friction coefficient, σ_n is the component of stress acting normal to the fault surface, τ_0 the cohesion and τ_f the limit shear stress. Contact elements have a zero thickness and are welded to the sides of viscoelastic elements (Parsons, 2002). Faults are permitted to slip during the entire time of the modelling. The fault friction coefficient has a value of 0.75.

Boundary conditions and loads

Tectonic loading is simulated by moving the eastern edge of the model at a constant rate of 2 cm yr^{-1} (Fig. 1). The western edge is constrained laterally ($V_x = 0$). The model base is free to slide laterally but cannot move vertically ($V_y = 0$). The free surface of the model is fully deformable. Before introduction of any boundary motion, the model is subjected to gravity for a time span of 10 ka so that it can become fully compressed under its own weight. The magma chamber pressure is at lithostatic equilibrium before any pressure variation is applied.

Simulation of pressure variation within a crustal magma reservoir

Displacements

We first tested the consequences of varying magma chamber pressure on the ground surface displacement and the offset on a nearby fault under general conditions of extension of 2 cm yr^{-1}. We simulated a pressure increase in the magma reservoir of 1, 5 or 10 MPa over 6 years, followed

by return to equilibrium within 1 year.

A magma pressure increase always produces uplift above the magma chamber, whereas a decrease in pressure produces subsidence. The rheology of the crust (oceanic or continental) does not influence significantly the vertical and horizontal displacements, or the Coulomb failure stress value. The fault dip influences ground deformation, especially in the case of horizontal displacements. The more steeply dipping the fault, the smaller the amount of horizontal displacement (Fig. 3). Within our suite of models, the horizontal displacement never exceeds 10 cm. The vertical displacement calculated above the magma chamber ranges between 10 and 20 cm (Fig. 3). The depth of the magma chamber plays a role. The deeper the reservoir, the smaller the amount of uplift (Fig. 3). While pressure increases linearly within the magma reservoir, the vertical displacement increases nonlinearly due to viscous relaxation near the magma reservoir. This effect can be observed also on the fault slip.

Fault slip

The slip on the normal fault due to the variation in reservoir pressure depends significantly on the position of the fault in relation to the magma reservoir (cf. Fig. 1B,C and Fig. 4). Depending on this factor, reverse or normal slip may occur on the fault in the case of pressure increase (Fig. 4). Pressure increase in a magma chamber located adjacent to the fault, laterally away (Fig. 4, curves A–D), produces a reverse slip on a given point of the fault at shallower depth than the magma chamber, whereas an identical pressure increase produces normal slip when the fault is located entirely above the magma chamber (Fig. 4E). The closer the fault is to the overpressure source, the smaller the amount of reverse slip (Fig. 4). This property is valid until the distance between the fault and the magma reservoir is under a critical distance that depends on the amplitude of the pressure variation and on the rigidity of the crust. The normal slip is associated with a decrease in pressure and frictional strength along the fault. In the case of reverse slip on a fault located laterally to the magma chamber, the

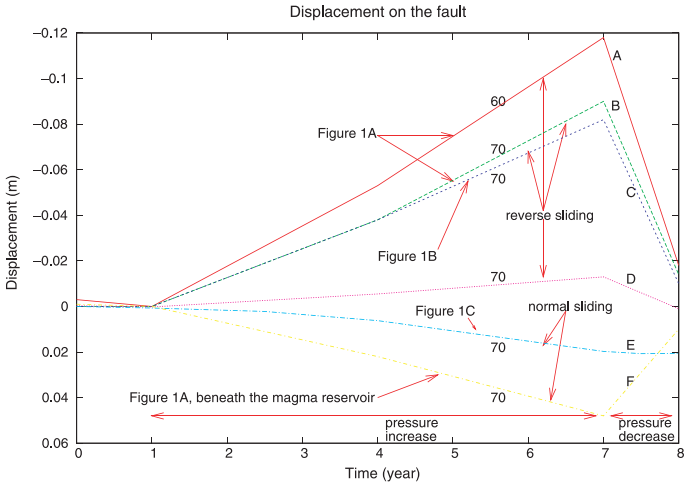

Fig. 3 Horizontal and vertical displacements at the topographic surface as a function of time. The magma chamber pressure is increased by 10 MPa over 6 years and decreased by 10 MPa over 1 year. The vertical displacement is calculated above the magma chamber nearby a fault with a dip of 70° for two different depths of the magma reservoir (3.5 and 6 km). The deeper is the magma reservoir, the smaller the vertical displacement. The vertical displacement is also calculated for two different dips of 70° and 60°. The more steeply is the fault, the greater the vertical displacement. The horizontal displacement is calculated at the right and at the left of the magma reservoir, located at a depth of 3.5 km, for two different fault dips (60° and 70°). The more steeply dipping the fault, the smaller the amount of horizontal displacement. Parameters used are the same as in Table 1. Magma chamber radius is 1 km. The fault is located at 2 km from the centre of the magma reservoir (Fig. 1A). The extension velocity is 2 cm yr^{-1}.

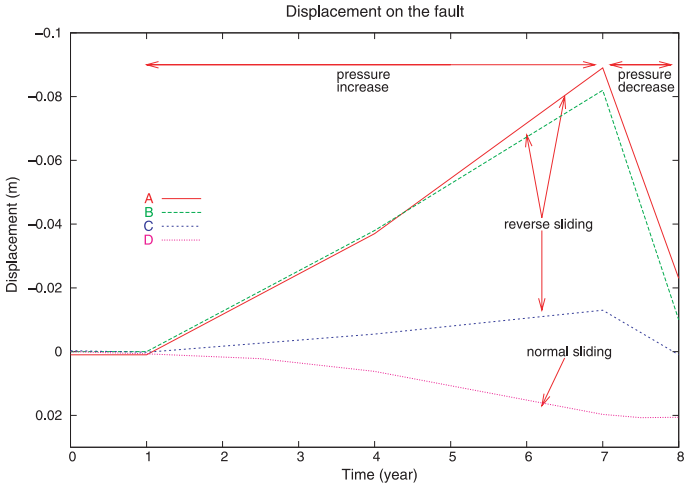

Fig. 4 Displacement of a point on the fault with time. The point is at shallower depth than the magma chamber (A–E). We compare the effect of fault location and dip on fault slip. (A) The geometry of the model is given in Fig. 1A, fault's dip is 60°. (B) The geometry is given in Fig. 1A, fault's dip is 70°. (C) The geometry is given in Fig. 1B, fault's dip is 70°. (D) The fault originates 1 km away from the magma chamber centre at 2.5 km depth, so the maximum depth of the fault is 2.5 km. (E) The geometry is given in Fig. 1C, fault's dip is 70°. (F) The geometry is given in Fig. 1A, fault's dip is 70°, slip on a point beneath the magma reservoir. The magma chamber pressure is increased by 10 MPa over 6 years and decreased by 10 MPa over 1 year. Positive (increase) displacement on the fault corresponds to normal slip and negative (decrease) displacement to reverse slip. Parameters used are the same as in Table 1. The 1-km-radius magma chamber is located at a depth of 3.5 km. Note the role of fault location in controlling the reverse/normal slip. The extension velocity is 2 cm yr^{-1}.

frictional strength on the fault increases, suggesting a seismogenic movement.

A pressure decrease within the magma reservoir will produce normal slip on faults located laterally to the magma chamber (Fig. 4, curves A–D) as well as when they originate above the magma reservoir (Fig. 4, curve E). The amplitude of the pressure variation does not affect the direction of offset but only the amplitude of the slip. The greater the amplitude of the pressure variation, the greater the fault displacement (Fig. 5). For a fault extending to great depth, the part of the fault at a depth equal or less than the chamber depth will experience reverse sliding in the case of magma pressure increase, whereas the deeper part of the fault plane will experience contemporaneously normal faulting (Fig. 4B,F). The situation is reversed for pressure decreases. Nevertheless, this fault geometry has a similar effect on fault displacement compared with the shorter fault (Fig. 4B,C). The slip on the fault is more sensitive to the distance between the magma reservoir and the fault than the fault length.

Coulomb stress variation around the magma reservoir

In the case of an increase in pressure of the magma reservoir, changes in Coulomb failure stress $\Delta\sigma_f$ indicate that the positive variations are most marked above and beneath the magma chamber (Fig. 6A,C,E). Therefore, we may expect seismicity and cracks to develop in this area.

The crust rheology, the magma reservoir depth, the amplitude of the pressure variation and the length of the nearby fault will influence the amplitude of the Coulomb failure stress change $\Delta\sigma_f$, but not the area where $\Delta\sigma_f$ is positive.

The Coulomb failure stress change $\Delta\sigma_f$ during chamber deflation is positive laterally offset from the extent of the deflation source, but negative above and beneath it (Fig. 6B,D,F). This result suggests that the deflation could produce seismicity and cracks that propagate into the crust laterally away from the magma reservoir.

Irrespective of whether pressure is increasing or decreasing, the dip of the nearby fault strongly influences

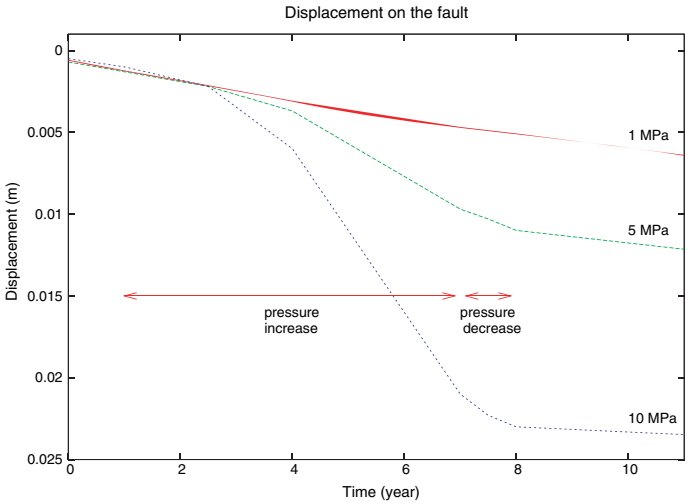

Fig. 5 Displacement on the fault above the magma chamber as a function of time. The magma chamber pressure is increased by 1, 5 or 10 MPa over 6 years and decreased by 1, 5 or 10 MPa over 1 year. The more is the pressure variation, the greater the fault displacement. The fault is located just above the magma chamber. This is the case C of Fig. 1. The dip of the fault is 70°. The throw on the fault is normal. Parameters of the model are those of Table 1. The 1-km-radius magma chamber is located at a depth of 3.5 km. The extension velocity is 2 cm yr^{-1}.

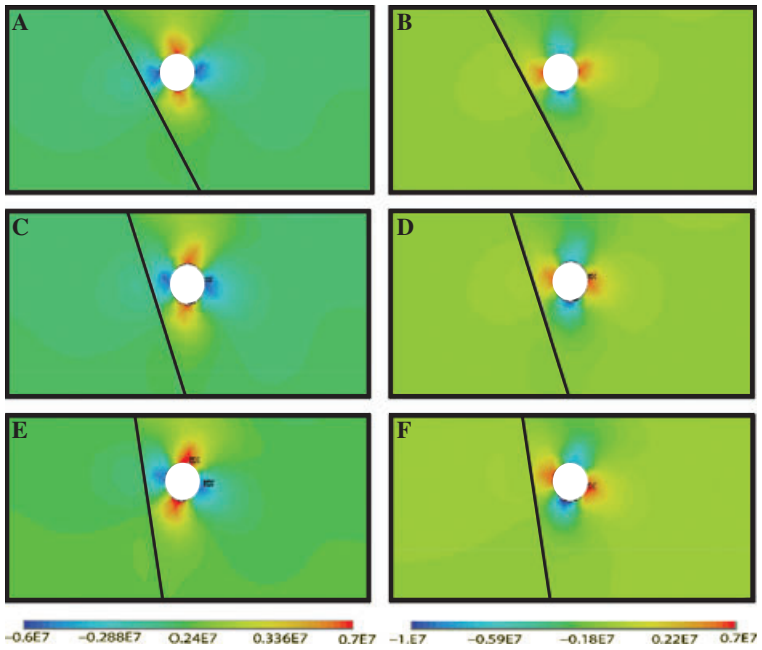

Fig. 6 Coulomb stress change (in Pa) calculated for a magma reservoir pressure increase (A, C and E) or decrease (B, D and F) nearby a fault. Various fault dips are tested (60°, 70° and 80°). The magma chamber pressure is increased by 10 MPa over 6 years and decreased by 10 MPa over 1 year. Higher positive values of Coulomb failure stress change $\Delta\sigma_f$ indicate expected location of seismicity. When pressure increases, the seismicity should occur above and beneath the magma reservoir. When pressure decreases, the seismicity should occur laterally offset from the extent of the magma reservoir. The dip of the fault strongly influences the location of the areas of positive and negative values of $\Delta\sigma_f$. Parameters used are the same as in Table 1. The 1-km-radius magma chamber is located at a depth of 3.5 km. The geometry is identical to Fig. 1A. The extension velocity is 2 cm yr^{-1}.

the location of the areas of positive and negative values of Coulomb failure stress change $\Delta\sigma_f$ (Fig. 6). The sub-planar area of positive $\Delta\sigma_f$ presents a 75–85° dip and makes an angle of 20–25° with the fault plane (Fig. 6).

Discussion and conclusion

Ground deformation and fault slip

The modelled surface deformations are in quantitative agreement with features observed in various volcanic areas (Tilling and Dvorak, 1993; Beauducel *et al*., 2000; Newman *et al*., 2001; Mann and Freymueller, 2003). Previous studies have already shown the role of faults in controlling the localization of ground deformation (De Natale and Pingue, 1993; De Natale *et al*., 1997). The role of boundary fractures to estimate the depth of the pressure source and surface deformations has been shown by Beauducel *et al*. (2004). Beauducel *et al*. (2004) showed that point source model in an elastic half space gave results not compatible with seismic and drill hole observations in Campi Flegrei. In the present study, we show that both the distance of the fault from the pressure source and the fault dip influence significantly the amplitude of the ground deformation (Fig. 3). Consequently, the pressure variation in the magma reservoir from ground deformation cannot be accurately quantified without having a good knowledge of the dip and position of faults in the area. This result is obtained with a discontinuity, which takes into account friction, into a viscoelastic lithosphere. The friction of the fault should be considered because it influences stress field, surface deformations and fault slip. We also took into account the viscosity of the lithosphere in our modelling. The viscosity of the lithosphere produces a nonlinear response on ground displacements and fault slip due to a linear pressure variation of the magma reservoir.

Concerning the slip on the fault, our results are in agreement with some previous studies as well as with certain field observations. Previous numerical and analogue modelling studies show that reverse slip is possible on faults near a magma reservoir in the case of reservoir inflation (Acocella *et al*., 2001; Walter and Troll, 2001; Troise *et al*., 2003) or due to the local stress induced by a nearby dyke (Gudmundsson and Loetveit, 2005). Another important result of our model concerns the possibility of normal slip on a fault above the inflation source. This last result is in accordance with some field observations: focal mechanisms with normal dip–slip motion have been observed above the magma reservoir during reservoir inflation at Campi Flegrei (Italy) nearby an inward dipping discontinuity (De Natale *et al*., 1995; Troise *et al*., 1997). Analogue modelling also suggests the possibility of normal slip on a fault located in the summital block above the magma reservoir during inflation (Acocella *et al*., 2001; Walter and Troll, 2001).

Coulomb stress variation, cracks and fault growth

The pattern of Coulomb failure stress change around a magma reservoir differs strongly during inflation compared with deflation. On the contrary, crust rheology (continental vs. oceanic), magma temperature and model boundary conditions (extension/no movement) have no significant effect on the sign of $\Delta\sigma_f$ or the distribution of positive $\Delta\sigma_f$.

The area of positive Coulomb failure stress change $\Delta\sigma_f$ (Fig. 6A,C,E), in which seismicity is supposed to occur preferentially, should be a zone with numerous cracks. Troise *et al*. (2003) pointed out that, in Campi Flegrei, seismicity with a normal dip component is coeval with episodes of fast uplift, being located above the magma chamber and strongly correlated with positive $\Delta\sigma_f$. Gray and Monaghan (2004) showed the possibility to obtain fracture growth above and laterally away from a magma chamber in an homogeneous rock without preexisting fault. In their study, the fracture growth was inclined or with more vertical angles depending on the extension rate. During reservoir inflation, we obtain an inclined planar area (~75–85°) with a positive Coulomb failure stress change $\Delta\sigma_f$ above the magma reservoir. This can be interpreted as reflecting the growth direction of a new fault or a permanent plexus of cracks (Fig. 7A). Studies on Kilauea volcano (Hawaii) show that the number of short-period earthquakes increases above and beneath the magma reservoir when surface inflation is observed (Tilling and Dvorak, 1993). Also our numerical models predict an increase of the Coulomb failure stress change in the region above and below the magma chamber, which suggests that earthquakes there are encouraged. The higher temperature below the magma reservoir reduces slightly the stress change beneath the reservoir. If we interpret the inclined plane of cracks above the magma chamber ($\Delta\sigma_f > 0$) as a fault, we would expect normal slip to occur because it is located just above the magma reservoir (see Fig. 4, curve E and Fig. 5).

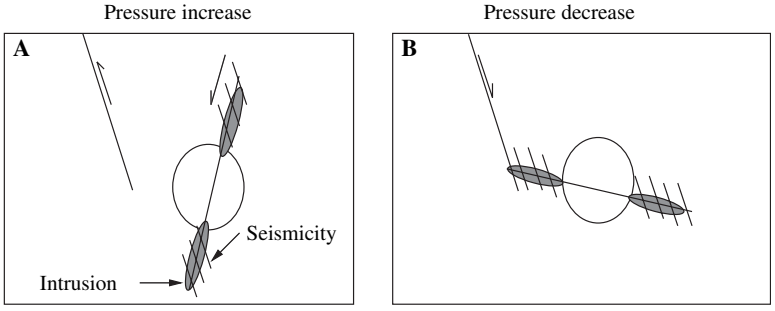

Fig. 7 Schematic interpretation of the influence of magma reservoir pressure variation with time. During the first stage (A), the pressure increases within the reservoir. The seismicity and cracking should occur preferentially in the hatched area. This area may constitute a preferential path for magma ascent. During the following second stage (B), the pressure decreases. The new area with $\Delta\sigma_f > 0$ is now subhorizontal and tends to intersect the fault plane. Magma injection within the subhorizontal cracked area depends on the magnitude of the pressure variation ΔP_m regarding $\Delta\sigma_{xy}$ (see text).

When the pressure of the magma reservoir decreases from an overpressured state (Fig. 7B), we observe an area of positive stress change $\Delta\sigma_f$, located laterally offset from the extent of the magma reservoir and at the same depth (Fig. 6B,D,F). Seismicity occurring laterally offset from the extent of the magma reservoir is often observed in volcanic areas (Tilling and Dvorak, 1993; Arnott and Foulger, 1994; Caplan-Auerbach and Duennebier, 2001; Newman *et al*., 2001; Clifton *et al*., 2002; Zobin, 2003). This seismicity is thought to be consecutive to magma intrusion (Toda *et al*., 2002), but could also be due to other processes such as hydrothermal activity (Almendros *et al*., 2002) or complex interactions between faults and pressure sources (Clifton *et al*., 2002). A few observations in the literature relate lateral seismicity to a decrease in magma reservoir pressure as suggested by our modelling. The occurrence of a change in location of seismicity around the magma reservoir before and after an eruption has been observed in the case of the 1989 Teishi Knoll activity (Japan), the May 1980 activity of Mt St Helens (USA), the New Tolbachik volcanoes (Russia) (Zobin, 2003) and the 1996 Loihi seamount collapse (Hawaii) (Caplan-Auerbach and Duennebier, 2001). Volcano–tectonic earthquakes related to shear failure were relocated laterally to the Loihi seamount during the beginning of a slow collapse, and have been clearly distinguished from long-period events associated with fluid or magma transport (Caplan-Auerbach and Duennebier, 2001). This is in agreement with our interpretation: our model suggests that seismicity may increase laterally offset from the extent of the magma reservoir due to a decrease in magma reservoir pressure.

Considering that the positive area of $\Delta\sigma_f$ corresponds to a cracked zone, the existing fault near the magma reservoir is likely to intersect the cracked zone (Figs 6B,D,F and 7B). The effect of this complex interaction on deformation needs to be detailed, but such a study falls outside the scope of this study. Nevertheless, the geometry of this intersection suggests a way of terminating the faults close to a magma reservoir.

Magma intrusion

In this section, we discuss the possible link between the calculated Coulomb failure stress change distribution around a magma reservoir and the injection of magma from such a reservoir into the surrounding rock. There are at least two ways in which magma can propagate into the crust. Tensile stress concentration is expected at specific areas around magma chambers especially in the case of increase in internal pressure (Gudmundsson, 1988). This leads to magma injection in dykes that trend perpendicular to the minimum compressive stress (mode I rupturing). Another possibility is that magma could propagate obliquely to the minimum compressive stress, if it invades a pre-existing fracture or fault that is misaligned with respect to the principal stress directions. We focus here on this second possibility because the magma reservoir can generate numerous faults along which the magma is able to propagate. There are three factors that could facilitate propagation of the magma along a fault (only one is necessary): (1) the fracture is nearly perpendicular to the minimum compressive stress; (2) the resolved shear stress on the fracture is small compared with the excess magma pressure; (3) the effective ambient pressure normal to the dyke is small compared with the tensile strength of the rock (Ziv *et al*., 2000).

Assuming that areas of rock damage (i.e. $\Delta\sigma_f > 0$ in our model) are similar to a faulted area, we would then expect magma to be injected preferentially along these directions. During magma reservoir inflation, sub-vertical weak zones are generated above and beneath the reservoir (Figs 6 and 7A). Such sub-vertical 'faults' are nearly perpendicular to the least compressive stress so that magma can propagate into them. The magma can propagate upwards from the magma chamber. This can also suggest a preferential location of hydrothermal fluid in the highly fractured rock area (i.e. $\Delta\sigma_f > 0$) above the magma chamber. The planar areas located beneath the chamber may also allow magma ascent from greater depth into the magma chamber. Alternatively, Caplan-Auerbach and Duennebier (2001) also suggest that the magma could drain into a deeper reservoir from a shallow reservoir. The propagation of magma may not be strictly vertical in a volcanic area close to a fault system: an analysis of the very-long-period waveform reveals the existence of a magma plumbing system dipping 80° below the Kilauea volcano (Hawaii) (Almendros *et al*., 2002).

Although magma reservoir deflation can be interpreted as a simple consequence of dyke intrusion, other processes can lead to the same results such as magma crystallization or thermal contraction (Mann and Freymueller, 2003). The deflation can facilitate magma propagation. During magma reservoir deflation, a sub-planar cracked zone is generated laterally to the magma chamber in a nearly horizontal plane (Fig. 7B). Conditions (1) and (3) for magma injection (Ziv *et al*. conditions) are not satisfied in this zone. Condition (2) may be satisfied at the beginning of deflation when the excess magma pressure is relatively high and the shear stress along the weak plane is small. In our modelling, this condition applies as long as the excess magma pressure ΔP_m exceeds ~2.5 MPa because, at the same time, the shear stress resolved on the direction of the 'fault' plane in the weak zone is relatively small (< 0.6 MPa). To our knowledge, such lateral propagation of magma has not been clearly documented.

References

Acocella, V., Cifelli, F. and Funiciello, R., 2001. The control of overburden thickness on resurgent domes: insights from analogue models. *J. Volcanol. Geoth. Res*., **111**, 137–153.

Almendros, J., Chouet, B., Dawson, P. and Bond, T., 2002. Identifying elements of the plumbing system beneath Kilauea Volcano, Hawaii, from the source locations of very-long-period signals. *Geophys. J. Int*., **148**, 303–312.

Angelier, J., Bergerat, F., Dauteuil, O. and Villemin, T., 1997. Effective tension–shear relationships in extensional fissure swarms, axial rift zone of north-eastern Iceland. *J. Struct. Geol*., **19**, 673–685.

Árnadóttir, X., Jónsson, S., Pedersen, R. and Gudmundsson, G.B., 2003. Coulomb stress changes in the south Iceland seismic zone due to two large earthquakes in June 2000. *Geophys. Res. Lett*., **30**, 1205. doi:10.1029/2002GL016495.

Arnott, S.K. and Foulger, G.R., 1994. The Krafla spreading segment, Iceland. 1. Three-dimensional crustal structure and the spatial and temporal distribution of local earthquakes. *J. Geophys. Res.*, **99**(B12), 23801–23826.

Beauducel, F., Cornet, F.-H., Suhanto, E., Duquesnoy, T. and Kasser, M., 2000. Constraints on magma flux from displacements data at Merapi volcano, Java, Indonesia. *J. Geophys. Res.*, **105**, 8193–8203.

Beauducel, F., De Natale, G., Obrizzo, F. and Pingue, F., 2004. 3-D modelling of Campi Flegrei ground deformations: role of caldera boundary discontinuities. *Pure Appl. Geophys.*, **161**, 1329–1344.

Bokelmann, G.H.R. and Silver, P.G., 2002. Shear stress at the base of shield lithosphere. *Geophys. Res. Lett.*, **29**, 2091. doi:10.1029/2002GLO15925.

Byerlee, J., 1978. The friction of rocks. *Pure Appl. Geophys.*, **116**, 615–626.

Caplan-Auerbach, J. and Duennebier, F.K., 2001. Seismicity and velocity structure of Loihi Seamount from the 1996 earthquake swarm. *Bull. Seismol. Soc. Am.*, **91**, 178–190.

Cattin, R., Doubre, C., de Chabalier, J.-B., King, G., Vigny, C., Avouac, J.-P. and Ruegg, J.-C., 2005. Numerical modelling of quaternary deformation and post-rifting displacement in the Asal-Ghoubbet rift (Djibouti, Africa). *Earth Planet. Sci. Lett.*, **239**, 352–367.

Cheng, L.Z., Mareschal, J.C., Jaupart, C., Rolandone, F., Gariepy, C. and Radigon, M., 2002. Simultaneous inversion of gravity and heat flow data: constraints on thermal regime, rheology and evolution of the Canadian shield crust. *J. Geodyn.*, **34**, 11–30.

Clifton, A.E., Sigmundsson, F., Feigl, K.L., Guomundsson, G. and Árnadóttir, T., 2002. Surface effects of faulting and deformation resulting from magma accumulation at the Hengill triple junction, SW Iceland, 1994–1998. *J. Volcanol. Geoth. Res.*, **115**, 233–255.

Cornu, T. and Bertrand, G., 2005. Numerical backward and forward modelling of the southern Upper Rhine Graben (France–Germany border): new insights on tectonic evolution of intracontinental rifts. *Quatern. Sci. Rev.*, **24**, 355–363.

De Natale, G. and Pingue, P., 1993. Ground deformations in collapsed caldera structures. *J. Volcanol. Geoth. Res.*, **57**, 19–38.

De Natale, G. and Zollo, A., 1986. Statistical analysis and clustering features of the Phlegraean fields earthquake sequence (May 1983–May 1984). *Bull. Seismol. Soc. Am.*, **76**, 801–814.

De Natale, G., Zollo, A., Ferraro, A. and Virieux, J., 1995. Accurate fault mechanism determinations for a 1984 earthquake swarm at Campi Flegrei caldera (Italy) during an unrest episode: implications for volcanological research. *J. Geophys. Res.*, **100**, 24167–24185.

De Natale, G., Petrazzuoli, S. and Pingue, F., 1997. The effect of collapse structures on ground deformations in calderas. *Geophys. Res. Lett.*, **24**, 1555–1558.

De Natale, G., Troise, C., Trigila, R., Dolfi, D. and Chiarabba, C., 2004. Seismicity and 3-D substructure at Somma-Vesuvius volcano: evidence for magma quenching. *Earth Planet. Sci. Lett.*, **221**, 181–196.

Doubre, C., 2004. Structure et mécanique des segments de rift volcano-tectoniques: application aux rift anciens (Ecosse, Islande) et actifs (Asal-Ghoubbet). Doctoral dissertation, Université du Maine, Le Mans, France.

Foulger, G.R., Du, Z. and Julian, B.R., 2003. Icelandic-type crust. *Geophys. J. Int.*, **155**, 567–590.

Foulger, G.R., Julian, B.R., Hill, D.P., Pitt, A.M., Marlin, P.E. and Shalev, E., 2004. Non-double-couple microearthquakes at Long Valley caldera, California, provide evidence for hydraulic fracturing. *J. Volcanol. Geoth. Res.*, **132**, 45–71.

Foulger, G.R., Natland, J.H. and Anderson, D.L., 2005. Genesis of the Iceland melt anomaly by plate tectonic processes. In: *Plates, Plumes and Paradigms* (G.R. Foulger, J.H. Natland, D.C. Presnall and D.L. Anderson, eds), Vol. 388, pp. 595–626. Geological Society of America, Boulder, CO.

Grant, J.V. and Kattenhorn, S.A., 2004. Evolution of vertical faults at an extensional plate boundary, southwest Island. *J. Struct. Geol.*, **26**, 537–557.

Gray, J.P. and Monaghan, J.J., 2004. Numerical modelling of stress fields and fracture around magma chambers. *J. Volcanol. Geoth. Res.*, **135**, 259–283.

Gudmundsson, A., 1988. Effect of tensile stress concentration around magma chambers on intrusion and extrusion frequencies. *J. Volcanol. Geoth. Res.*, **35**, 179–194.

Gudmundsson, A. and Brenner, S.L., 2004. How mechanical layering affects local stresses, unrests, and eruptions of volcanoes. *Geophys. Res. Lett.*, **31**, L16606. doi:10.1029/2004GL020083.

Gudmundsson, A. and Loetveit, I.F., 2005. Dyke emplacement in a layered and faulted rift zone. *J. Volcanol. Geoth. Res.*, **144**, 311–327.

Gudmundsson, A., Marti, J. and Turon, E., 1997. Stress fields generating ring faults in volcanoes. *Geophys. Res. Lett.*, **24**, 1559–1562.

Hill, D.P., Pollitz, F. and Newhall, C., 2002. Earthquake–volcano interactions. *Phys. Today*, , 41–47.

Hofton, M.A. and Foulger, G.R., 1996. Postrifting anelastic deformation around the spreading plate boundary, north Iceland. 1. Modeling of the 1987–1992 deformation field using a viscoelastic Earth structure. *J. Geophys. Res.*, **101**, 25403–25421.

Huismans, R.S., Podladchikov, Y.Y. and Cloething, S., 2001. Transition from passive to active rifting: relative importance of asthenospheric doming and passive extension of the lithosphere. *J. Geophys. Res.*, **106**, 11271–11291.

Karato, S.-I. and Wu, P., 1993. Rheology of the upper mantle: a synthesis. *Science*, **260**, 771–778.

King, G.C.P., Stein, R. and Lin, J., 1994. Static stress changes and the triggering of earthquakes. *Bull. Seismol. Soc. Am.*, **84**, 935–953.

Mann, D. and Freymueller, J., 2003. Volcanic and tectonic deformation on Unimak Island in the Aleutian Arc, Alaska. *J. Geophys. Res.*, **108**, 2108. doi:10.1029/2002JB001925.

Micarelli, L., Moretti, I. and Daniel, J.M., 2003. Structural properties of rift-related normal faults: the case study of the Gulf of Corinth, Greece. *J. Geodyn.*, **36**, 275–303.

Newman, A.V., Dixon, T.H., Ofoegbu, G.I. and Dixon, J.E., 2001. Geodetic and seismic constraints on recent activity at Long Valley caldera, California: evidence for viscoelastic rheology. *J. Volcanol. Geoth. Res.*, **105**, 183–206.

Nostro, C., Stein, R., Cocco, M., Belardinelli, M.E. and Marzocchi, W., 1998. Two-way coupling between Vesuvius eruptions and southern Apennine earthquakes, Italy, by elastic stress transfer. *J. Geophys. Res.*, **103**, 24487–24504.

Parsons, T., 2002. Post-1906 stress recovery of the San Andreas fault system calculated from three-dimensional finite element analysis. *J. Geophys. Res.*, **107**. doi:10.1029/2001JB001051.

Pascal, C. and Cloething, P.L., 2002. Rifting in heterogeneous lithosphere: interferences from numerical modeling of the northern North Sea and the Oslo Graben. *Tectonics*, **21**, 1060. doi:1029/2001TC901044.

Stein, R., 1999. The role of stress transfer in earthquake occurrence. *Nature*, **402**, 605–609.

Tilling, R.I. and Dvorak, J.J., 1993. Anatomy of a basaltic volcano. *Nature*, **363**, 125–132.

Toda, S., Stein, R. and Sagiya, T., 2002. Evidence from the AD 2000 Izu islands earthquake swarm that stressing rate governs seismicity. *Nature*, **419**, 58–61.

Troise, C., 2001. Stress changes associated with volcanic sources: constraints on Kilauea rift dynamics. *J. Volcanol. Geoth. Res.*, **109**, 191–203.

Troise, C., De Natale, G., Pingue, F. and Zollo, A., 1997. A model for earthquake generation during unrest episodes at Campi Flegrei and Rabaul calderas. *Geophys. Res. Lett*., **24**, 1575–1578.

Troise, C., Pingue, F. and De Natale, G., 2003. Coulomb stress changes at calderas: modelling the seismicity of Campi Flegrei (southern Italy). *J. Geophys. Res*., **108**, 2292. doi:10.1029/2002JB002006.

Turcotte, D.L. and Schubert, G., 2002. *Geodynamics*, 2nd edn. Cambridge University Press, Cambridge, 456 pp.

Walter, T.R. and Amelung, F., 2004. Influence of volcanic activity at Mauna Loa, Hawaii, on earthquake occurrence in the Kaoiki seismic zone. *Geophys. Res. Lett*., **31**, doi:10.1029/2003GL019131.

Walter, T.R. and Troll, V.R., 2001. Formation of caldera periphery faults: an experimental study. *Bull. Volcanol*., **63**, 191–203.

van Wijk, J.W. and Cloething, S.A.P.L., 2002. Basin migration caused by slow lithospheric extension. *Earth Planet. Sci. Lett*., **198**, 275–288.

Wilks, K.R. and Carter, N.L., 1990. Rheology of some continental lower crustal rocks. *Tectonophysics*, **182**, 594–604.

Ziv, A., Rubin, A.M. and Agnon, A., 2000. Stability of dike intrusion along preexisting fractures. *J. Geophys. Res*., **105**, 5947–5961.

Zobin, V.M., 2003. *Introduction to Volcanic Seismology*. Elsevier, Amsterdam, 290 pp.

Received 7 February 2006; revised version accepted 25 July 2006

